

## Design of Accordion Spring for Roller One-Way Clutches

WANG Jiaxuan<sup>1</sup>, LIU Cheng<sup>1\*</sup>, GUO Meng<sup>1,2\*</sup>, YAN Qingdong<sup>1</sup>, WEI Wei<sup>1</sup>

1. School of Mechanical Engineering, Beijing Institute of Technology, Beijing 100081, P.R. China;

2. Yangtze Delta Region Academy, Beijing Institute of Technology, Jiaxing 314000, P.R. China

(Received 2 November 2022; revised 16 March 2023; accepted 21 June 2023)

**Abstract:** Generally, a one-way clutch uses coil springs to push and energize the rollers. However, clutches with coil springs are hard to assemble. Moreover, using coil springs, the rollers are prone to bear eccentric load during operation, which decreases the reliability of the clutch. In order to increase the manufacturability and durability of the one-way clutch, an accordion spring is proposed. First, the equivalent spring constant is derived using energy method. After that, a rigid-flexible coupling finite element model is established to analyze and discuss the piecewise linear property of the spring's stiffness characteristic. Based on the equal stiffness assumption, a parametric design method that uses length as constraints and load as boundary conditions is further proposed to design the spring. Finally, several accordion springs are made to carry out an experiment, which validates the accuracy of the theoretical model, the finite element analysis (FEA) model and the parametric design method.

**Key words:** accordion spring; roller one-way clutch; equivalent spring constant; finite element analysis (FEA)

**CLC number:** TH122

**Document code:** A

**Article ID:** 1005-1120(2023)03-0264-09

### 0 Introduction

Roller one-way clutch is an essential element in an integrated torque converter. It is composed of an outer race, an inner race, several rollers and springs. When unlocked, the spring presses the roller towards the narrow part of the wedge to keep the roller in stable contact with the inner or the outer race, and at the same time, ensure uniform bearing of each roller. A certain type of one-way clutch with coil springs is shown in Fig.1(a), which results in a complicated structure of the outer race, making it difficult to manufacture and assemble. Therefore, the spring is optimized by replacing original coil springs with accordion springs.

As shown in Fig.1(b), the accordion spring has a simple structure and is easy to assemble, which helps to simplify the outer race and make the whole clutch assembly lighter. Accordion springs are widely used in the roller one-way clutches of passenger cars<sup>[1]</sup>.

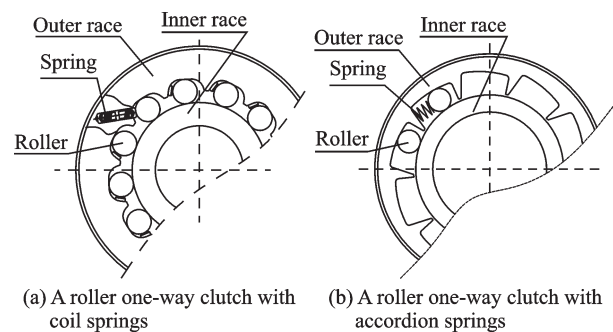


Fig.1 Different springs used in roller one-way clutches

The application of accordion springs in foreign countries started early. They have fully developed the technology and formed a relatively complete series of products. Baumle et al.<sup>[2]</sup> designed a roller type one-way clutch with accordion springs and a roller cage. It is a typical structure of one-way clutches in automatic transmission. One end of the spring is fixed on the cage, and the other has the same curvature as the roller. The roller is confined in the cage by the spring, so the roller has a relatively stable working position. The thickness of the ac-

\*Corresponding authors, E-mail addresses: liucheng@bit.edu.cn; guomeng826025@163.com.

**How to cite this article:** WANG Jiaxuan, LIU Cheng, GUO Meng, et al. Design of accordion spring for roller one-way clutches[J]. Transactions of Nanjing University of Aeronautics and Astronautics, 2023, 40(3):264-272.

<http://dx.doi.org/10.16356/j.1005-1120.2023.03.003>

accordion spring is about 0.051—0.076 mm<sup>[3]</sup>. Man-  
kar et al.<sup>[4]</sup> proposed an accordion spring and its  
parametric design method, then they calculated the  
equivalent stress when the spring was compressed  
by finite element analysis. They pointed out that the  
thickness of the metal sheet/leaf should be larger  
than 0.4 mm for springs with small stiffness. Law-  
son<sup>[5]</sup> used composite progressive accordion springs  
on the vehicle suspension system. The spring had  
piecewise-linear stiffness by changing the angle and  
number of bends on spring spokes.

At present, there are a few researches on the  
equivalent stiffness of accordion springs. Qiu et al.<sup>[6]</sup>  
considered the accordion spring as a flexible connec-  
tion mechanism or a flexible hinge. They designed a  
variable pitch folding flexure hinge (PFFH), de-  
rived its equivalent stiffness by using the Moore inte-  
gral, and analyzed its piecewise linear stiffness char-  
acteristics. A formula for calculating the stiffness of  
the U-shaped leaf spring is given in the national stan-  
dard<sup>[7]</sup>. Based on that, Peng et al.<sup>[8]</sup> modified the  
section of the U-shaped spring, and analyzed the in-  
fluence of structure parameters, such as spring an-  
gle, arm length and thickness, on the spring con-  
stant. But Peng's boundary conditions are quite dif-  
ferent from those of springs in a one-way clutch, so  
it is inappropriate to directly apply his conclusions to  
the one-way roller clutch<sup>[9-11]</sup>. Accordion springs  
have been widely studied and applied in MEMS.  
However, MEMS springs mainly bear tensile and  
torsional loads<sup>[12]</sup>, and they are very small, usually  
on a micrometer scale. Compared with clutch  
springs, they are much smaller and flatter. Mean-  
while, the accordion spring of one-way clutches is  
compressed in most working conditions. When the  
deformation is too large, the spring pieces will con-  
tact with one and another, which makes the stiff-  
ness characteristics more complex, and quite differ-  
ent from that of the MEMS springs. So, there is an  
urgent need for a general method to guide the design  
of accordion springs.

The present study will therefore focus on the  
design of the accordion spring used in one-way  
clutch and calculation of the spring constant. In the  
study, we first propose an accordion spring and de-

rive its equivalent stiffness equation based on energy  
method. The finite element model of the spring is es-  
tablished which helps to analyze the piecewise-linear  
characteristic of the spring constant. To facilitate the  
design, we propose a parametric design method of  
the accordion spring, which optimizes the accordion  
spring under constraints of size and performance. An  
experiment is carried out to verify the proposed mod-  
el.

## 1 Structure and Modelling of Ac- ordion Spring

### 1.1 Structure of accordion spring

The profile of the proposed accordion spring is  
shown in Fig.2. The spring has  $n$  ( $\geq 4$ ) segments  
and it is composed of two basic elastic units, as  
shown in Fig.3. The elastic unit composed of a  
straight section and a semicircle is called type I  
spring (S I), and the segment with semicircles/  
arcs at both ends is defined as type II spring (S II).  
The free length of the spring is  $L_0$ , the length of the  
straight section of S I is  $L_1$ , and the angle of the arc  
section of S II is designated as  $\alpha$ . The inner radius  
of each arc is  $r$ . The metal sheet/leaf has a thickness  
of  $b$  and a width of  $h$ . The Young's modulus of the  
material is designated as  $E$ . The part of the spring

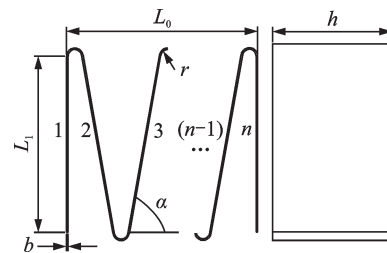


Fig.2 Structure of accordion spring

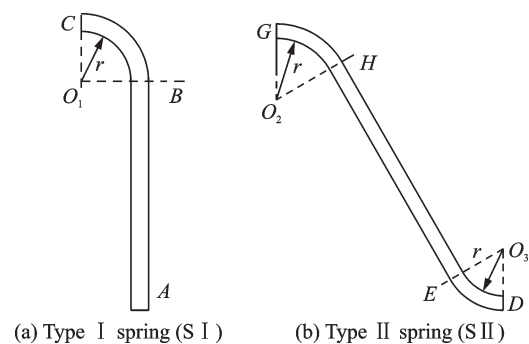


Fig.3 Two basic elastic elements

that contacts with the outer race is called the “tail”, and one that contacts with the roller is called the “head”. Both tail and head are S I springs.

## 1.2 Theoretical model of the equivalent stiffness

Due to the structural of the spring, the stiffness of the accordion spring in the compression process is nonlinear, and it changes with different contact conditions. Fig.4 shows three typical stages of the spring when compressed. When the deformation is small, the basic elastic elements do not contact with each other, and each basic unit is compressed freely. At this time, the equivalent spring constant is  $k_1$ . With the increase of deformation, when the head and tail, both of which are S I springs, contact with the adjacent S II spring at the same time, the equivalent spring constant dramatically increases to  $k_2$ . The stiffness is approximately infinite under complete compression. The energy method is used to calculate the compression stiffness  $k_1$ .

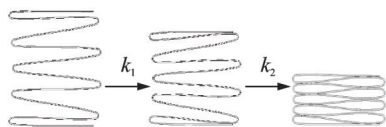


Fig.4 Process of spring compression

To simplify the movement of the roller and to better establish the theoretical mode, a few assumptions are made as follows.

When designing the one-way clutch, the spring is only allowed to be compressed and stretched axially. This is usually guaranteed by using a slot, a spring cage or a spring supporter. It can be seen from Fig.5 that when the spring is installed inside the chamber, its tail is considered fixed. Therefore, to simplify the mechanical model, the sliding between the spring and the wall is ignored, which is equivalent to fixing<sup>[13]</sup> the arc of the tail to the wall.

The center line of the spring is in line with that of the roller, so  $F$  is exerted on the middle of the spring's head when the clutch is locked, as shown in position A in Fig.5. When the clutch is unlocked, the roller tends to move towards the wider part of the chamber due to centrifugal force. The faster the clutch rotates, the further the roller goes. The roller stops at position B where the spring is compressed to its limit. The maximum displacement of the roll-

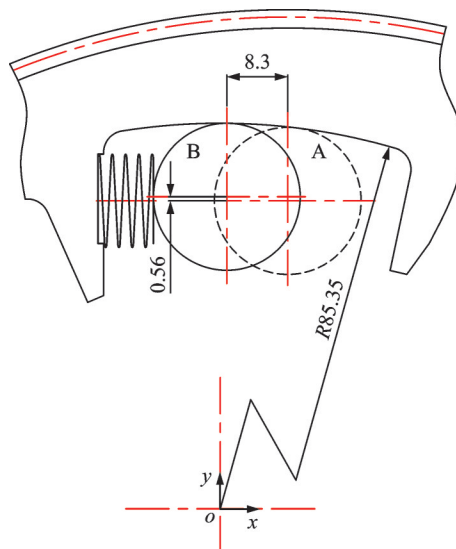


Fig.5 Displacement of the roller

er's centroid along  $y$ -axis is about 0.56 mm, which is relatively small compared to its  $x$ -axis displacement (8.3 mm). Considering that curvature of the chamber is as small as  $0.012 \text{ mm}^{-1}$ , it's reasonable to simplify the movement of the centroid as a rectilinear one. Since  $F$  is exerted on the middle of the head in the preliminary stage of unlocking (Fig.5, position A), assume that it always acts on the middle.

The gravity of the spring itself and friction between contact faces are not included in calculation. Fig.6 shows the simplified mechanical model of the spring under compression. The rotation of the interfaces of two elastic elements is very small and can be ignored, so a simplified mechanical model of two basic elastic elements can be obtained. The mechanical model is shown in Fig.7.

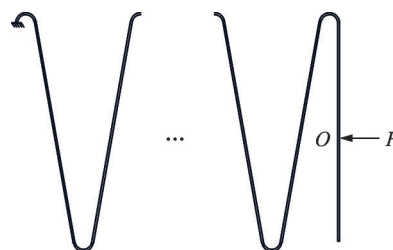


Fig.6 Simplified mechanical model of spring

In this case, the normal and shear force generated by the spring are very small, which can be ignored. When calculating the strain energy, only the bending couple is considered<sup>[14]</sup>. The bending couple  $M_i^{(1)}$  and strain energy  $V_1$  of S I are

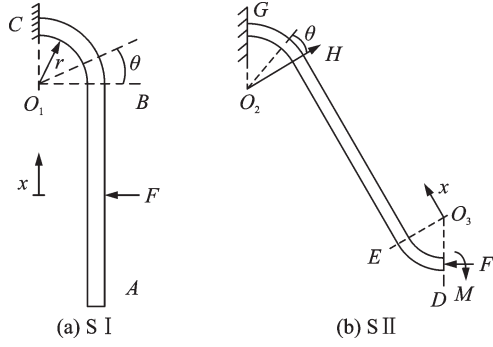


Fig.7 Simplified mechanical model of basic units

$$\begin{cases} M_1^{(1)}(x) = Fx & 0 \leq x \leq \frac{L_1}{2} \\ M_2^{(1)}(\theta) = \frac{FL_1}{2} + Fr\sin\theta & 0 \leq \theta \leq \frac{\pi}{2} \end{cases} \quad (1)$$

$$V_1 = \int_0^{L_1/2} \frac{(M_1^{(1)}(x))^2}{2EI} dx + \int_{BC} \frac{(M_2^{(1)}(\theta))^2}{2EI} ds \quad (2)$$

where  $I$  is the moment of inertia of the cross section of the spring, for a rectangular section  $I = hb^3/12$ , and  $M_1^{(1)}, M_2^{(1)}$  are the bending couples of the straight section and the circular section respectively.

The bending couple  $M_j^{(i)}$  and strain energy  $V_2^{(i)}$  of the  $i$ th ( $i = 2, 3, \dots, n-1$ ) S II are

$$\begin{cases} M_1^{(i)}(\theta) = T_{i-1} \pm 2Fr\sin^2\frac{\theta}{2} & 0 \leq \theta \leq \alpha \\ M_2^{(i)}(x) = Fx\sin\theta_0 \pm T_{i-1} \pm 2Fr\sin^2\frac{\alpha}{2} & 0 \leq x \leq L_2 \\ h(\theta) = r\cos(\alpha - \theta) - r\cos\alpha & 0 \leq \theta \leq \alpha \\ L_2 = \frac{2L_1}{\sin\alpha} + \frac{2\left(r + \frac{h}{2}\right)}{\tan\alpha} \\ M_3^{(i)}(\theta) = T_{i-1} \pm Fh(\theta) \pm FL_2\sin\alpha \pm 2Fr\sin^2\frac{\alpha}{2} & 0 \leq \theta \leq \alpha \end{cases} \quad (3)$$

$$V_2^{(i)} = \sum_{j=1}^3 \int_s \frac{(M_j^{(i)}(\theta))^2}{2EI} ds \quad (4)$$

In the formula, when  $i$  is an odd number, “ $\pm$ ” is a plus sign, and when  $i$  is an even number, it is a minus sign.  $T_{i-1}$  is the reaction force exerted by the  $(i-1)$ th section to the  $i$ th section. In particular,  $T_0 = M_2^{(1)}(\pi/2)$ .  $M_1^{(i)}, M_3^{(i)}$  are the bending couples of the arc sections, and  $M_4^{(i)}$  is the bending couple of the straight section.

According to the assumed conditions, only the circular section actually takes part in the deformation of S I at the tail, and its bending couple  $M_3(\theta)$  and strain energy  $V_3$  are

$$M_3(\theta) = M_3^{(n-1)}(\alpha) - 2Fr\sin^2\frac{\theta}{2} \quad (5)$$

$$V_3 = \int_s \frac{(M_3(\theta))^2}{2EI} ds \quad (6)$$

To sum up, the total strain energy  $V$  of the whole spring is

$$V = V_1 + V_3 + \sum_{k=2}^{n-1} V_2^{(k)} \quad (7)$$

According to Castigliano’s second theorem, the displacement generated along the  $F$  direction at point  $O$  is

$$\Delta = \frac{\partial V}{\partial F} \quad (8)$$

Therefore, according to Hooke’s law, when each segment is freely compressed, the coefficient of stiffness  $k_1$  of an accordion spring with  $n$  sections in the direction of pressure  $F$  can be found as

$$k_1 = \frac{F}{\Delta} \quad (9)$$

In this study, a 10-segment accordion spring is designed with metal sheet/leaf thickness  $b$  of 0.1 mm, spring width  $h$  of 56 mm, the radius  $r$  of 0.45 mm,  $L_1$  of 11.6 mm, and the inclination  $\alpha$  of 80°. Parameters of the accordion spring here can make sure the force exerted on rollers is the same with that using coli springs. The material used here is alloy steel, density  $\rho = 7850 \text{ kg/m}^3$ , Young’s modulus  $E = 206 \text{ GPa}$ , Poisson’s ratio  $\mu = 0.3$ , and yield strength  $\sigma_y = 205 \text{ MPa}$ . The stiffness  $k_1$  of the spring under the axial compression is 0.601 N/mm according to Eqs.(1—9).

## 2 Finite Element Analysis of the Compression Process

A finite element model of the spring is established in ANSYS Workbench to further understand the whole process of compression. The model consists of a spring, a base and a roller. Compared with the spring, the roller and the base have higher stiffness and small contact surface deformation, so they can be considered as rigid bodies. The roller is only

partially modeled to save computational resources. The thickness of the spring section is small, so linear shell element Shell181 is used for meshing with the maximum mesh size no larger than 0.6 mm. In the compression process, each basic spring element will contact with the one next to it successively, so frictional contact is defined between all the contact faces. In the simulation, the friction coefficient is 0.15 and the normal stiffness factor of the contact surface is 0.1<sup>[15]</sup>.

It is important to specify how the roller moves when compressed. The FEA model simulates the following two processes: (1) Pre-compression of the spring when assembled; (2) compression of the spring when the clutch is unlocked. This pre-compression is along the  $x$ -axis, so it can be simulated by a rectilinear motion of the roller. When the clutch is unlocked, due to the small displacement of the roller in  $y$ -direction<sup>[16]</sup> and the small curvature of the chamber, shown in Fig.5, the curvilinear movement of the roller can be simplified into a rectilinear one. Considering the two processes, we decide to simplify the motion of the roller into a rectilinear one, so it can only move in the  $x$ -direction in the simulation<sup>[17-18]</sup>. The roller applies a pressure of 18 N in the  $x$ -direction in 1 s. The base is fixed to the ground as a support. Fig.8 shows the finite element model.

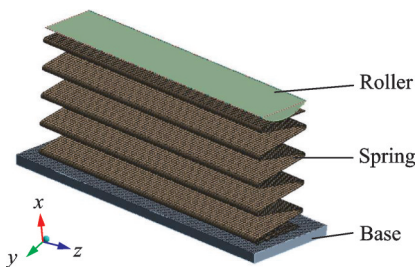


Fig.8 Finite element model of spring compression

The roller's displacement in the  $x$ -direction is extracted as shown in Fig.9. A complete compression of the spring consists of three stages:  $OA$ ,  $AB$  and  $BE$ . Stage  $OA$  is the free compression of the spring where the basic elastic units are not in contact with each other and the force-displacement characteristics is linear. In this stage the spring has an

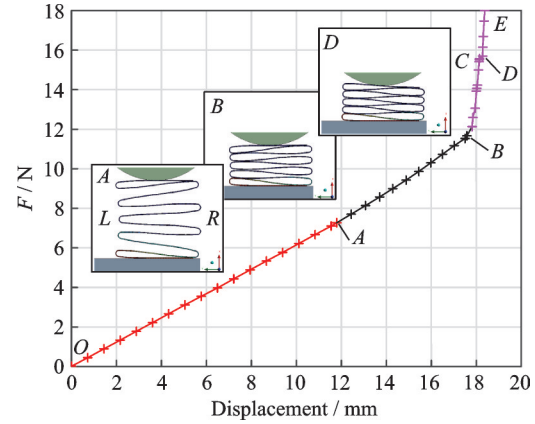


Fig.9 Longitude displacement of the roller

equivalent spring constant of  $k_1$ . At point  $A$ , the tail and the head, both of which are S I units, contact with their adjacent S II units, and the spring stiffness increases to  $k_2$ . With the increase of the longitudinal compression, the lateral ( $y$ -direction) displacement of the spring also gradually increases due to the difference between  $k_1$  and  $k_2$ . When the spring is compressed to point  $B$ , all the circular segments on the left of the spring contact with each other at the same time. In stage  $BE$ , the circular segments on the right side gradually come into contact. Starting from point  $C$ , the tail slides slightly in the  $y$ -axis under the elastic force generated by the lateral deformation, and the sliding ends at point  $D$ . This sliding makes the head rotate clockwise along the  $z$ -axis, which causes force  $F$  to deviate from the middle of the head (namely point  $O$ ) and results in an equivalent longitude displacement of the spring. The spring is fully compressed at point  $E$ .

Using the least square approximation to fit the piecewise-linear relationship between the force and the displacement of  $O-A-B$  yields

$$F = \begin{cases} 0.613U + 0.00550 & 0 \leq U \leq x_A \\ 0.749U - 1.62 & x_A < U \leq x_B \end{cases} \quad (10)$$

where  $F$  is the roller force, and  $U$  the displacement of roller in the  $x$ -axis direction, which equals to the longitudinal deformation of the spring. The difference in the spring constants is trivial ( $k_1 = 0.613$ ,  $k_2 = 0.749$ ), and it largely depends on the structure of the spring. The stiffness of the free compression section, namely  $k_1$ , is 0.613 N/mm.

In summary, in  $OA$  and  $AB$  stages the spring

has a linear stiffness, respectively. The rotation of S I unit in these stages is small, so it can be considered that force  $F$  acts at the middle of the head.  $BE$  stage involves the contact of several basic elastic units and the sliding of the tail, leading to a more complicated force-displacement relationship and a larger spring constant. At the end of the stage, the spring is almost completely compressed, and the von-Mises stress in the circular section of S II is much higher. To avoid plastic deformation and abrupt change of spring force, it's preferable to make the spring work in  $OA$  and  $AB$  stages, namely the linear stages, as much as possible.

### 3 Parametric Design of Accordion Spring

The parametric design methodology can relieve researchers from the workload of iterative design and has been widely used in the design, optimization and manufacture of products<sup>[19-20]</sup>. When designing the accordion spring, one must know the load  $F_w$  exerted by the roller and the corresponding length  $L_w$  in advance. For a given load  $F_w$ , there can be infinite  $L_w$  because equivalent stiffness varies from spring to spring. However, it is difficult to determine which stage the accordion spring works in. Since the difference between  $k_1$  and  $k_2$  is small, it is reasonable to assume that the spring has constant stiffness  $k_1 = k_w = F_w / (L_0 - L_w)$ . To further ensure the designed spring has an appropriate length, the displacement  $\Delta$  derived from Eqs.(1-8),  $(L_0 - L_w)$ -to- $L_0$  ratio  $\Delta'$  and the length-to-thickness ratio  $z$  are used as dimensional constraints. Under the constraints mentioned above, a method for optimal design of the spring is therefore proposed. The constraints are as follows.

#### (1) Constraint on the length of compression

The theoretical result of longitudinal ( $x$ -direction) deformation  $\Delta$  must match the actual deformation  $U_w = L_0 - L_w$  in actual practice. It is acceptable that the relative error between  $\Delta$  and  $U_w$  is within 3%, which is

$$e_r = \left| \frac{U_w - \Delta}{\Delta} \right| \times 100\% \leq 3\% \quad (11)$$

where  $L_0$  is the free length of the spring, and  $U_w$  the

longitudinal deformation of the spring when compressed.

#### (2) Constraint on the length $L_w$

The ratio of the spring deformation to its total length should be moderate. When compressed, the spring's deformation should not be too long in case that it has plastic deformation or works in  $BE$  stage, and it should not be too short in case of an excessive stiffness. Depending on the situation,  $z$  varies from 0.3 to 0.6, which is

$$0.3 \leq \Delta' = \frac{U_w}{L_0} \leq 0.6 \quad (12)$$

where  $U_w = L_0 - L_w$ .

#### (3) Constraint on the length-to-thickness ratio

Define the length-to-thickness ratio  $z$  of a spring as the ratio of its free length  $L_0$  to its thickness  $b$ . The larger the length-thickness ratio is, the longer and thinner the whole spring will be. The length-thickness ratio significantly affects the lateral ( $y$ -direction) stiffness of the spring and increases the inclination of the spring's head in free compression, thus affecting the accuracy of the theoretical calculation results. Fig.10 shows the effect of the length-to-thickness ratio on the accuracy of  $k_1$  derived by theoretical calculation. It is noticeable that the accuracy of theoretical model decreases as  $z$  increases. Although  $e_r$  is still within 10% for a spring with larger  $z$ , it has noticeable lateral displacement during the longitudinal compression (Fig.11). A spring with large  $z$  will rub with the inner race, which reduces its durability. In order to improve the accuracy of the theoretical model, the length-to-thickness ratio should be no larger than 240, which is

$$z = \frac{L_0}{b} \leq 240 \quad (13)$$

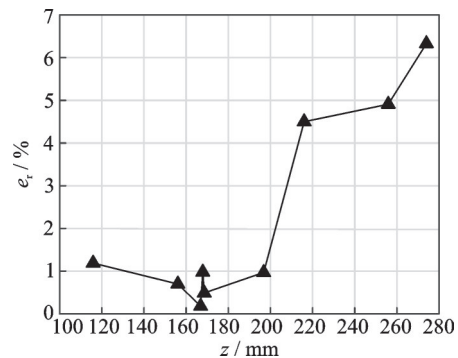


Fig.10 Effect of  $z$  on the accuracy of theoretical model

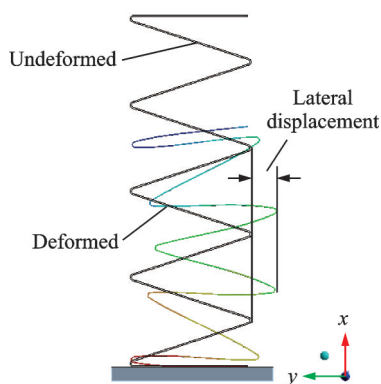


Fig.11 Lateral displacement

The design procedure is shown in Fig.12. For a given outer race, the width  $h$  is equal to the total length of the rollers in one chamber, so it is a constant. Metal sheet/leaf thickness  $b$  varies in a small range, so it can be determined by experience or the thickness of the available material. It is also reasonable to regard it as a constant. Therefore, among all the parameters,  $L_1$ ,  $r$  and  $\alpha$  need to be specifically designed. As an example, we will explain in detail about how to determine the exact  $L_1$  and  $r$  to illustrate the optimization procedure. At the outset, one has to specify the range of  $L_1$  and  $r$  and their increments, either from database or by experience. After that,  $\alpha$  should be decided by the length of the wedge on the outer race to make sure that the free length of the spring is always smaller than the length of the

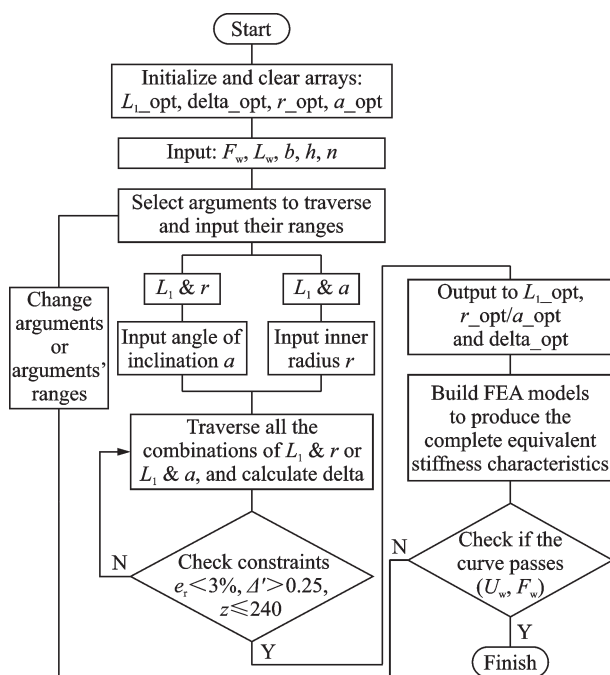


Fig.12 Flow chart of the spring optimization procedure

wedge. For each parameter combination of  $L_1$  and  $r$ , calculate the displacement  $\Delta$ , and output the parameter combination and the corresponding  $\Delta$  that satisfy dimensional constraints to arrays  $L_{1\_opt}$ ,  $r\_opt$  (or  $2\_opt$ , if the angle  $2$  is optimized) and  $\delta_{opt}$ , respectively. Based on this, the complete stiffness characteristic of the spring can then be obtained by finite element analysis, which is also used as a reference to adjust the parameters to meet working conditions. Compared with selecting all parameters by experience, the design method based on dimension constraint provides better guidance.

## 4 Experiment and Discussion

A series of springs are made to conduct the experiment on a stiffness test device. These springs are only tested in their linear compression stages. Pushing or pulling the handle can control the displacement of the roller and the force  $F$  exerted on the spring, as shown in Fig.13. When  $F$  is 1, 2,  $\dots$ , 11 N, respectively, record the corresponding displacement, designated as  $U_{ei}$ . We calculate the mean value of all the tests and use linear least square approximation to determine regression coefficients.

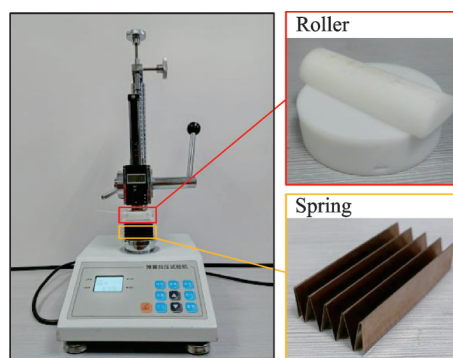


Fig.13 Stiffness test devices and the accordion spring

At each displacement  $U_{ei}$  measured in the experiment, FEA model (Eq. (10)) and theoretical model (Eqs. (1—9)) are both used to calculate the corresponding force  $F_e$  and its relative error  $e_r$ . The results are shown in Fig.14. The experiment and simulation are well-matched, with  $e_r$  being about 6.2% for small compressions and less than 3% for large ones.

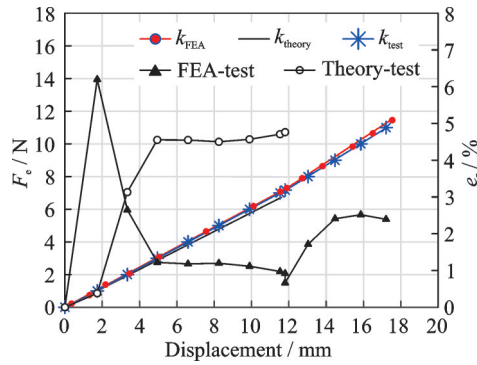


Fig.14 Comparison of  $k_i$  &  $e_r$  among FEA model, theoretical model and tests

Spring constants predicted by different methods are shown in Table 1. The FEA model predicts  $k_1$  with high accuracy, but the error enlarges when predicting  $k_2$ . Even though, the relative error is acceptable for engineering use, we think the FEA model is reasonably reliable. The theoretical model can also predict  $k_1$  (0.601 N/mm) with high accuracy, with the maximum relative error of  $F_e$  lower than 6% compared with the FEA model. This means the theoretical model can also meet the requirement for engineering use.

**Table 1 Comparison of spring constants derived by FEA and experiments**

Spring constant/ (N•mm <sup>-1</sup> )	Theory	FEA	Experiment
$k_1$	0.601	0.613	0.610
$k_2$		0.749	0.708

## 5 Conclusions

(1) We first propose an accordion spring used in roller one-way clutches and then derive its equivalent spring constant using energy method. Then we establish a finite element model of the spring to analyze and discuss the force-displacement characteristics of the spring when it is compressed. FEA model shows that the spring has a piecewise continuous stiffness characteristic. Finally, the FEA and theoretical model are verified by experiments. Results show that both FEA model and theoretical model are accurate enough.

(2) Based on the theoretical calculation, to speed up the design process, a parametric design

method is proposed to optimize the spring under given constraints. We propose the length-thickness ratio  $z$  as an important indicator to evaluate the accuracy of the theoretical model.

## References

- [1] ZHU Jingchang. Torque convertor design and calculation[M]. Beijing: National Defense Industry Press, 1991. (in Chinese)
- [2] BAUMLE R. One-way roller clutch accordion spring with stabilizer: AU6994387A[P]. 1987-09-17.
- [3] MERRELL R, BOWIE E. Roller one-way clutches for today's passenger car automatic transmissions[J]. SAE Transactions, 1967, 76: 434-452.
- [4] MANKAR S, ASHRITH S, SENGUPTA B. Design of accordion spring for automotive application[J]. International Journal of Engineering Research and Technology, 2017, 6(4): 712-715.
- [5] LAWSON R. Composite progressive accordion spring: GB2367876[P]. 2004-03-24.
- [6] QIU Lifang, LIU Yuansong, YU Yue, et al. Design and stiffness analysis of a pitch-varying folded flexure hinge (PFFH)[J]. Mechanism and Machine Theory, 2021, 157: 104187.
- [7] CHENG Daxian. Handbook of mechanical design [M]. Beijing: Chemical Industry Press, 2016. (in Chinese)
- [8] PENG Yueyang, HUANG Zhihui, JIANG Xutao, et al. Research on the impact of structure parameters on the stiffness and mechanical property of a special-shaped leaf spring[J]. Machinery, 2022, 60(5): 43-47. (in Chinese)
- [9] SUN Chengcheng, JI Yaping, WANG Xiaoxia, et al. Study on stiffness of MEMS spring with variable section width in W-type[J]. Modern Manufacturing Technology and Equipment, 2021, 57(11): 20-22, 27. (in Chinese)
- [10] HE Guang, SHI Gengchen. Comparative study on stiffness characterization of planar S & W-form micro-springs based on MEMS[J]. Chinese Journal of Sensors and Actuators, 2008(2): 288-291. (in Chinese)
- [11] HE Guang, SHI Gengchen. Study on stiffness characterization of planar W-form micro-springs based on MEMS technology[J]. Journal of Beijing Institute of Technology, 2006(6): 471-474. (in Chinese)
- [12] ZHANG Yu, PAN Wu. Design and analysis of a MEMS horizontal torsion micro mirror with folded springs[J]. Optics and Precision Engineering, 2005 (S1): 81-85. (in Chinese)



- [13] XU Yiwei, CHU Changxiang, GAO Xiao, et al. Stress and fatigue analysis of the leaf spring in an overrunning clutch based on Workbench[J]. Machinery, 2015, 53(4): 40-43. (in Chinese)
- [14] HAN Bing. Tutorials on mechanics of materials[M]. Beijing: Publishing House of Electronics Industry, 2013. (in Chinese)
- [15] WANG Ziquan, HUANG Wei, CHEN Weinan, et al. Optimization design and comprehensive evaluation of screw contact of space battery based on ANSYS[J]. Transactions of Nanjing University of Aeronautics and Astronautics, 2021, 38(3): 474-483.
- [16] QING Mingshu, WANG Shenghua, XU Dibin, et al. Development design of multi-roller overrunning clutch for motorcycle engine[J]. Motorcycle Technology, 2021(6): 32-37. (in Chinese)
- [17] XU Yiwei. Optimization design and experiment research on overrun clutch of planetary gearbox[D]. Liuzhou: Guangxi University of Science and Technology, 2015. (in Chinese)
- [18] FAN Lin. Overrunning clutch with leaf springs[J]. Machinery, 1996, 34(10): 12.
- [19] WANG Hongxian, HOU Yu, ZHANG Ming, et al. Sensitivity analysis and optimization of geometric parameters of a new fluid bag buffer mechanism on buffering performance[J]. Transactions of Nanjing University of Aeronautics and Astronautics, 2022, 39(5): 569-583.
- [20] WANG Jie, ZHAO Miaodong, MAO Jianxing. Parametric modeling system for cooling turbine blade based on feature design[J]. Transactions of Nanjing University of Aeronautics and Astronautics, 2020, 37(5): 758-767.

**Authors** Mr. WANG Jiaxuan received his B.S. degree in mechanical engineering from Beijing Institute of Technology in 2021 and he is currently pursuing the M.S. degree in Beijing Institute of Technology. His research interests include hydraulic transmission and reconfigurable wheel-tracked system.

Dr. LIU Cheng received his Ph.D. degree from Beijing Institute of Technology in 2015 and he is currently an associate professor at Beijing Institute of Technology. His research interests include vehicle hybrid technology, fluid transmission and transient cavitation.

Dr. GUO Meng received his Ph.D. degree from Beijing Institute of Technology in 2022 and he is currently a post-doctoral at School of Mechanical Engineering, Beijing Institute of Technology. His research interests include machine design, fluid transmission and control, and transient cavitation.

**Author contributions** Mr. WANG Jiaxuan designed the study, established the theoretical and FEA model, conducted the analysis, interpreted the results and wrote the draft. Dr. LIU Cheng contributed to the supervision, investigation and discussion of the study, and revised and edited the draft. Dr. GUO Meng revised and edited the draft, and helped a lot with the experiments. Prof. YAN Qingdong contributed to the project administration and funding acquisition of the study. Prof. WEI Wei contributed to the supervision and funding acquisition of the study. All authors commented on the manuscript draft and approved the submission.

**Competing interests** The authors declare no competing interests.

(Production Editor: WANG Jing)

## 单向联轴器折叠弹簧设计方法

王嘉轩<sup>1</sup>, 刘城<sup>1</sup>, 郭猛<sup>1,2</sup>, 闫清东<sup>1</sup>, 魏巍<sup>1</sup>

(1.北京理工大学机械与车辆学院,北京 100081,中国; 2.北京理工大学长三角研究院(嘉兴),嘉兴 314000,中国)

**摘要:**目前国内普遍采用的单向联轴器压紧机构为传统的圆柱弹簧,其结构复杂、装配难度大,且使用过程中易出现偏载,降低联轴器可靠性。为提高单项联轴器可制造性和寿命,本文提出一种折叠弹簧,采用卡式第二定理推导出其等效刚度理论计算公式,并建立了刚柔耦合有限元模型,对弹簧的压缩过程进行数值模拟,研究分析了其分段线性的刚度特性。提出了折叠弹簧参数化设计方法,在给定工作载荷和工作长度的情况下,以等刚度假设为前提,压缩长度、工作段占比和长厚比为约束条件,能够实现弹簧结构参数的快速优化设计。最后,研制了折叠弹簧样件,进行弹簧刚度试验,验证了理论模型、仿真模型及设计方法的正确性。

**关键词:**折叠弹簧;单向联轴器;弹簧等效刚度;有限元分析